Available online at www.sciencedirect.com

jmr&t Journal of Materials Research and Technology

journal homepage: www.elsevier.com/locate/jmrt

Original Article

Design and development of defect rich titania nanostructure for efficient electrocatalyst for hydrogen evolution reaction in an acidic electrolyte

Murugesan Praveen Kumar [a], *Govindhasamy Murugadoss* [b,*], *Ramalinga Viswanathan Mangalaraja* [c,h], *Prabhakarn Arunachalam* [d], *Manavalan Rajesh Kumar* [e], *Unalome Wetwatana Hartley* [f], *Sunitha Salla* [g], *Jothiramalingam Rajabathar* [d], *Zeid A. ALOthman* [d,*], *Tariq ALTalhi* [h]

[a] *CSIR-Central Electrochemical Research Institute (CSIR-CECRI), Karaikudi, 630003, India*
[b] *Centre for Nanoscience and Nanotechnology, Sathyabama Institute of Science and Technology, Chennai, 600119, India*
[c] *Laboratory of Advanced Ceramics and Nanotechnology, Department of Materials Engineering, University of Concepción, Concepción, Chile*
[d] *Chemistry Department, College of Science, King Saud University, P.O. Box: 2455, Riyadh 11451, Saudi Arabia*
[e] *Institute of Natural Science and Mathematics, Ural Federal University, Yekaterinburg, 620002, Russia*
[f] *Mechanical and Process Engineering Department, Sirindhorn International Institute of Technology, King Mongkut's University of Technology North Bangkok, Bangkok, 10800, Thailand*
[g] *Department of Chemistry, Sathyabama Institute of Science and Technology, Chennai, 600119, India*
[h] *Department of Chemistry, College of Science, Taif University, P.O. Box 11099, Taif 21944, Saudi Arabia*

ARTICLE INFO

Article history:
Received 30 March 2021
Accepted 26 July 2021
Available online 8 August 2021

Keywords:
Defect rich titania nanostructure
Electrocatalyst
Electrochemical anodization and cathodization method
Hydrogen evolution reaction (HER)
Water splitting

ABSTRACT

Cost-effective, efficient and stable electrocatalyst for water splitting in the acidic electrolyte medium has been developed. The acidic electrolyte could be a support for the high purity hydrogen production via water splitting. Accordingly, we have prepared the defect-rich titania nanostructure via electrochemical anodization and cathodization routes using the titanium plate, which showed highly effective and durable electrocatalyst of hydrogen evolution reaction (HER) in an acidic medium. This hybrid compound showed a low onset potential of −0.17 V for HER with a current density of −150 mA cm^{-2} in 1 M H_2SO_4. Moreover, the stability test has been performed with the defect-rich titania nanostructure as cathode for 6 h in the two electrodes system.

* Corresponding authors.
E-mail addresses: murugadoss_g@yahoo.com (G. Murugadoss), zaothman@ksu.edu.sa (Z.A. ALOthman).
https://doi.org/10.1016/j.jmrt.2021.07.119

1. Introduction

Fossil fuels such as coal and petroleum have been sources of energy for the past hundreds of years. Owing to the persistent consumption of these fuels, there is a chance that it may not be available in the future. So, there comes a need to search for an alternate fuel source, which should be abundant and also economical. Globally, the researchers are looking for green energy to substitute the current fossil fuels and make a sustainable energy source for the future. To the continuous energy needful, the natural gas of hydrogen becomes efficient energy for replacing the primary non-renewable energy sources [1–3]. Furthermore, a very less percentage of hydrogen is available directly in nature. However, it can be obtained via various methods like stem reforming, gasification, pyrolysis, algae and water splitting [4–8]. Among them, hydrogen production via a hydrogen evolution reaction (HER) by electrochemical water splitting method is one of the foremost technologies [8]. Platinum (Pt) has been the noblest electrocatalyst for the HER, and its electronic conductivity is very good when compared to any other metal [9,10]. To cope with the excellent properties of Pt, we need to develop a good electrocatalyst that is almost identical to Pt [11–22]. Here, the interesting properties of titania depend on its structural variety [23] and conductivity area from semiconducting to metallic by creating the oxygen defect (O/Ti stoichiometry) [24,25] with various nanostructures such as nanoparticles, nano-plates and nanoclusters. Among the all nanostructures, the titania-based nanoclusters have a great attention for HER due to their unique properties such as high surface area with controllable pore size, high hydrogen adsorption energy and that could be successfully bounded by proton impart. Those properties of nanoclusters could be enhanced by the reaction activity of titania in terms of the exchange current density for HER in an acidic medium. Consequently, the generating defect sites resulting in a vacancy-induced disconcertion and overlay the vacancy channels via vacancy-strain coupling, vacancy–vacancy, vacancy–electron interactions, and characteristics improvement in electronic features. We have further encountered the technique of electrochemical water splitting using one of the righteous electrocatalysts called the defect-rich 'titania' nanostructure [26–28]. The defect-rich titania nanostructure has been a non-noble catalyst for electrochemical studies and it has good electronic conductivity and stability in both the alkaline and acidic media next to platinum [29–32]. The defect rich titania nanoclusters are subjected to anodization [33,34] and immediate cathodization [35,36] in the acidic electrolyte (H_2SO_4) for various intervals of time. During this process, the oxygen vacancies were created due to the lattice-strained in titania nanostructure. Furthermore, the defect-rich titania nanoclusters were prepared with controlled size and improving surface activity. Hence, the HER (hydrogen evolution reaction) are monitored in an acidic medium. The defect-rich sites are formed with nanoclusters due to the oxygen vacancies created, which form the HER's active sites. Therefore, the electrocatalytic property of the defect-rich titania nanostructure electrode is modified, and from the linear sweep voltammetry (LSV) studies, we have observed the curve close to that of the noble platinum anode. Further, the electronic conductivity, lattice structures, and morphology also showed that the cathodic reduced defect rich titania nanostructure could be used as a promising electrocatalyst for HER. The results obtained from the Tafel slope by electrochemical studies revealed that the onset potential of the defect-rich titania nanostructure in an acidic medium lay in the range of −0.17 V and the current density of −150 mA cm^{-2}. The continuous stability test, which was carried out for 6 h, confirmed that the defect-rich titania nanostructure had highly stable. Thus, the defect-rich titania nanostructure had performed as an excellent catalyst that closed to the performance of the platinum catalyst.

2. Experimental section

2.1. Materials

Titanium was obtained from Alfa Aesar, India. Sulphuric acid, nitric acid, hydrofluoric acid, potassium hydroxide, and sodium carbonate were acquired from Sigma Aldrich. All the chemicals were of pure analytic grade and used as received without any modifications.

2.2. Apparatus and material characterization

The electrochemically prepared defect-rich titania nanostructure phases were characterized by using a PANalytical PW3040/60 X'pert PRO X-ray diffractometer with a Cu target ($\lambda = 0.154$ nm). The surface morphology was examined using a SUPRA 55 field emission scanning electron microscope (FE-SEM), which operated at an acceleration voltage of 5–30 kV. The two- and three-dimensional surface topographies of the as-synthesized defect-rich titania nanostructure plates were analyzed using atomic force microscopy (AFM, 5500 Series, Agilent Technologies, US). The electrochemical experiments were conducted at room temperature employing an electrochemical workstation (SP-150, Biologic science instruments, France). The oxygen vacancies were investigated using electron paramagnetic resonance (EPR, EMx Plus X Band, BRUKER BIOSPIN, Germany). A classical three-electrodes setup with platinum as the counter electrode, a saturated calomel as the reference electrode and the cathodized defect-rich titania nanostructure as the working electrode was used. The Raman spectra were recorded for the prepared samples using LabRAM HR Evolution Laser-Raman spectrometer with an excitation wavelength of 514 nm from Oxxius laser source (100 mW). The morphology of prepared samples was investigated by using TEM (a FEITECNAI).

2.3. Fabrication of defect-rich TiO_2 nanostructure

The titanium plates were surface cleaned using an etching solution. The composition of the etching solution consisted of 25 mL of distilled water, 20 mL of nitric acid and 5 mL of hydrofluoric acid. The plates were thoroughly etched to remove the thin deposits, especially the oxide films, as they were exposed to the atmosphere. The plates were dipped into the acidic solution for around 2 min. The etched plates were sonicated to remove unwanted impurities. The well-etched plates were sonicated for 10 min with a soap solution and subsequently on the distilled water for another 10 min. The

defect-rich TiO_2 preparation is schematically illustrated in Scheme 1.

2.4. Anodization

The sonicated plates were then subjected to an anodization process in a 0.5 M sulphuric acid electrolyte, and the Pt was used as a cathode. While the plate acted as an anode, a voltage of 10 was applied for the anodization process utilizing a potentiometer. The process was carried out for different time durations at 1, 3, 5 and 7 min for several plates. During the anodization, the titanium plates were transformed into a defect-rich TiO_2.

2.5. Cathodization

Once the anodization process has been completed, the samples were subsequently subjected to cathodization process under similar conditions. This process was carried out to improve the surface of the sample for more electronic conductivity. Flowsheet 1 displayed a step of electrode preparation to obtain defect-rich TiO_2 nanostructure.

3. Results and discussion

3.1. Structural analysis

The X-ray diffraction (XRD) is a non-destructive method that offers the complete evidence about the crystallographic structure, chemical composition, and physical features of the materials. Fig. 1A shows the phase transformation of as-prepared TiO_2 nanostructure concerning the time variation on anodization and cathodization processes. The XRD peaks of TiO_2 nanostructure are appeared at the 2θ values of 35.9 (1 1 1), 39.1 (2 0 0), 41.0 (1 1 1), 53.7 (2 1 1), 63.7 (3 1 0), 71.3 (3 1 1), 76.8 (2 0 2) and 78.1° (2 1 2) which are corresponded to TiO, Ti, Ti, Ti, Ti, Ti, TiO and Ti phases, respectively, for 1 min cathodizationTi substrate as shown in Fig. 1A (a) (JCPDS file no. 00-029-1361). Fig. 1A (b), (c) and (d) represent the intensity of major XRD peaks at 39.1° and 71.3° (Ti) for 3, 5, and 7 min cathodization process, which is considerably less compared to 1 min. The result indicates that the metallic surface is converted to oxide surface (TiO) and it has been confirming by the presence of a peak at 41° with high intensity. Furthermore, the XRD pattern of TiO_2 nanostructure for 7 min displays that the less peak intensity at 71.3° (Ti), which confirms the formation of TiO at the surface of plate is higher percentage compared to other less time cathodization process. The investigated XRD result clearly demonstrates that the stoichiometric amorphous TiO_2 is reconstructed by restructures in the form of a non-stoichiometric crystalline phase with enriching defects by the cathodic reduction process. Fig. 1A (e) shows the XRD peak of 7- and 9-min samples. The peak of 71.3° was appeared in higher intensity for 9 min compared to 7, which represents increasing crystallinity of metallic Ti. From these results, we optimized 7 min can be suitable for HER activity.

3.2. Surface morphology

The surface morphology of TiO_2 nanostructure was investigated by FE-SEM. The anodized defect-rich titania (TiO_2) nanostructure clearly shows the surface roughness features shown in Fig. 2. Fig. 2a shows the FE-SEM image of TiO_2 nanostructure for 1 min cathodization sample, which appears a well uniformed porous morphology on the surface of

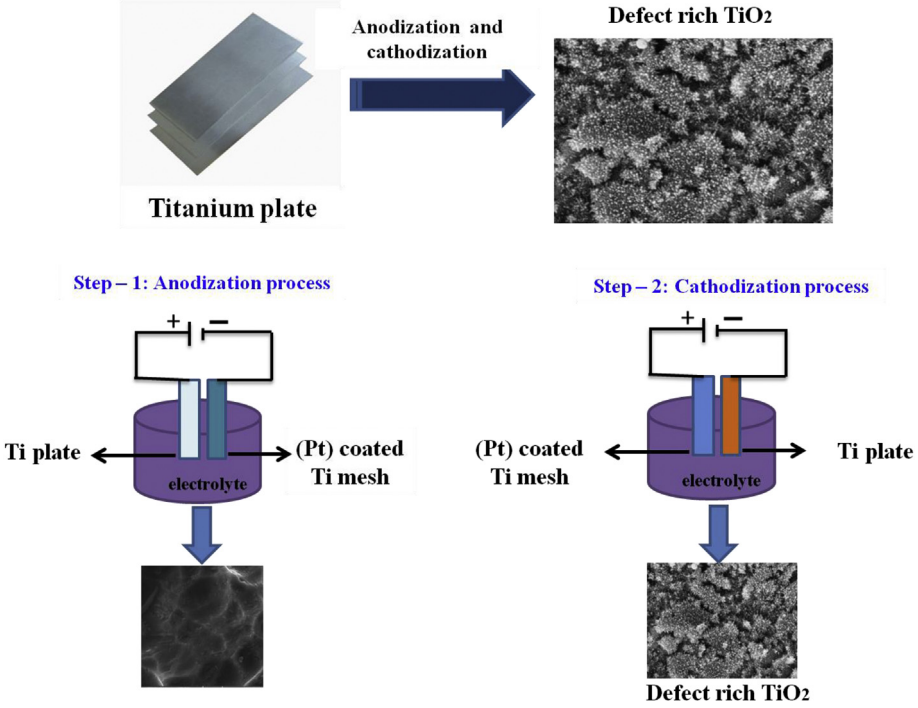

Scheme 1 – Scheme demonstration of synthesis of defect rich titania nanostructure by electrochemical cathodization method.

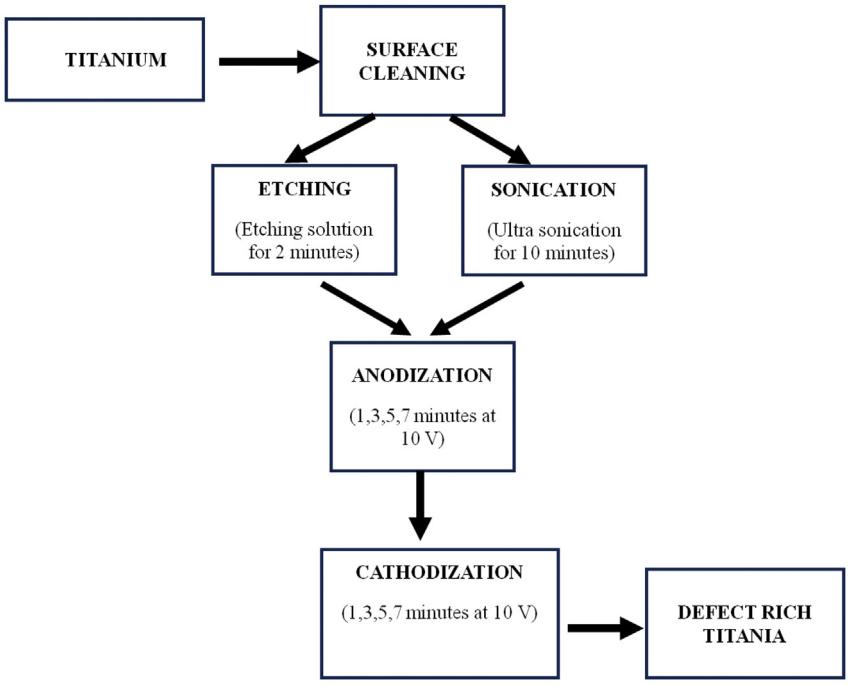

Flow sheet 1 – The details of experimental steps.

Ti plate. Further, the Ti plate was applied for cathodization process with various time conditions. The surface-modified TiO_2 nanostructures are shown in Fig. 2b, c and d for cathodization at different time durations of 3, 5 and 7 min, respectively. The morphology of 3 and 5 min cathodization samples revealed the initial status of growth of Ti clusters, as shown in Fig. 2b and c. Moreover, the defect-rich titania increases the significant roughness and the morphological change has been observed in a 7 min cathodization sample, as shown in Fig. 2d that depicts the possibility of highly electrocatalytic features for HER. Fig. 2d displays a homogeneous dispersion of nanoclusters on a porous matrix after cathodic treatment of the defect rich titania nanostructure. The metallic titania nanoparticles are embedded on the microporous titania nanostructure during the cathodization method, facilitating both active metallic sites and voids spaces for the electrochemical reaction and consequent hydrogen exclusion from the surface of the electrode. Fig. 2e exhibits the homogeneous dispersion of TiO_2 nanoclusters destruction on the titanium metal surface. Furthermore, the cathodization time has optimized for the destruction of the surface morphology, and the FESEM image confirms the surface modification for 9 min in Fig. 2e. Fig. 2f shows the TEM and SAED pattern of 7 min defect rich titania nanostructure sample. The surface morphology of sample is clearly showing that formation of nanoclusters, which is a further confirmation and SAED pattern exhibits the polycrystalline present in the 7 min sample. FESEM images for before and after HER study of 7 min cathodization is provided in Fig. S1. Furthermore, the surface area (10.950 m^2/g), pore volume (0.017 cc/g) and pore size (21.015 Å) of 7 min sample was carried out using BET analysis as shown Fig. S2. This surface changes support to increase the mass transformation between the electrode surface and the electrolyte solution during HER. The additional information is provided in the supplementary information. To further analysis composition and structural information, Raman study was performed. The discussion of the study is presented in supplementary information (Fig. S3).

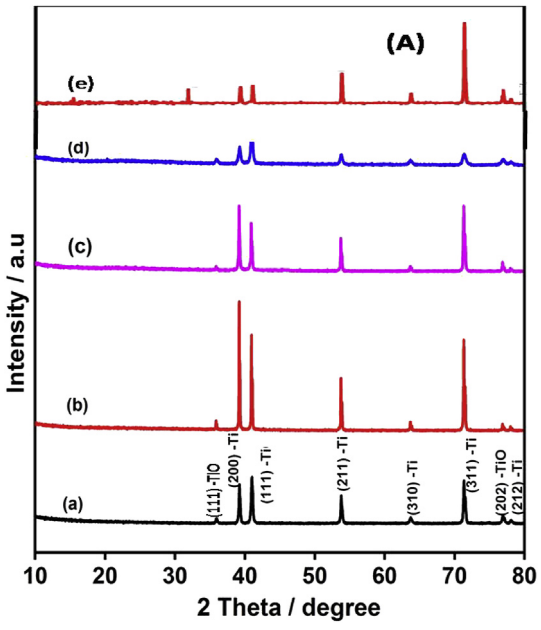

Fig. 1 – (A) XRD patterns for (a) 1, (b) 3, (c) 5 (d) 7 and (e) 9 min cathodized defect rich titania nanostructure.

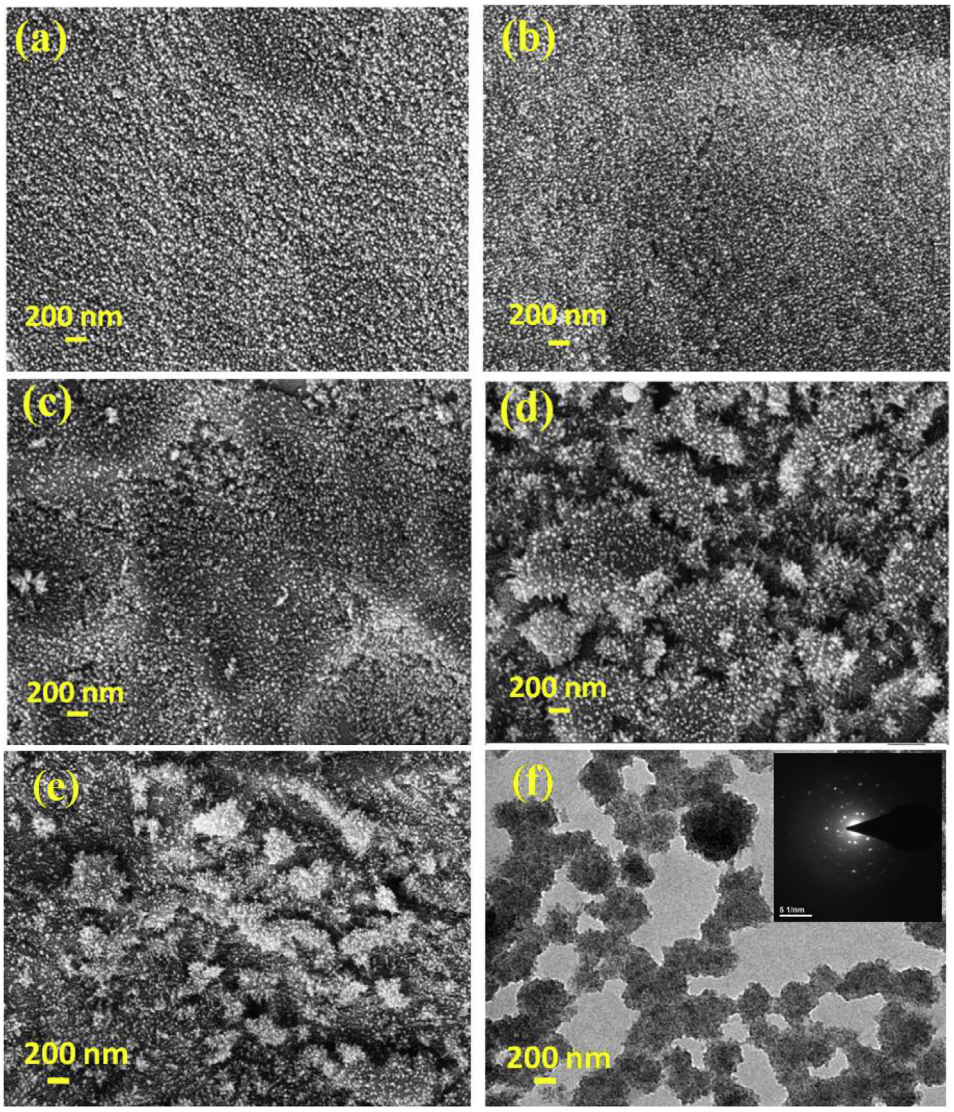

Fig. 2 – FE-SEM images of (a) 1, (b) 3, (c) 5, (d) 7 and (e) 9 min cathodized defect rich titania nanostructure samples. (f) TEM image of 7 min defect rich titania nanostructure samples and corresponding SAED pattern provided (insert).

3.3. *Energy dispersive X-ray analysis*

The elemental composition of the defect-rich titania nanostructure cathodized for different time durations was carried out using energy dispersive X-ray analysis (EDAX) and shown in Fig. 3. The EDAX spectra of the cathodization of the defect-rich titania nanostructure for 1, 3, 5 and 7 min. The obtained spectra confirm the presence of Ti and O. Further, the atomic% and weight% of Ti and O are as follows, which represents the reduction in the percentage of O with respect to the various times (Fig. 4).

3.4. *AFM analysis*

The atomic force microscope (AFM) is a very-high-resolution kind of scanning probe microscopy. The AFM is used to regulate a surface sample's roughness or evaluate a crystal growth layer's thickness. Fig. 5a shows that the cathodized sample for 1 min is homogeneously smooth and contributes less catalytic activity than the other cathodized sample. Fig. 5b shows the high rough surface of 7 min compared to the anodized sample. The topographies of the three- and two-dimensional AFM images (25 μm × 25 μm in size) are shown in Fig. 5. The roughness factor values are 0.990 nm and 0.499 μm for 1 and 7min samples, respectively, as shown in Fig. 5a1 and b1. The surface roughness of 7 min is higher than 1 min, which is revealed that the roughness is increasing based on cathodization time.

3.5. *XPS study*

The surface chemical states of the samples were determined by X-ray photoelectron spectroscopy (XPS) spectra. Fig. 6a shows that the Ti high resolution XPS spectra of 1 min cathodization sample peaks are appeared at 458.6 eV (Ti^{3+}) and 459.2 eV (Ti^{4+}) for $Ti2p_{3/2}$ level, whereas $Ti2p_{1/2}$ level peaks

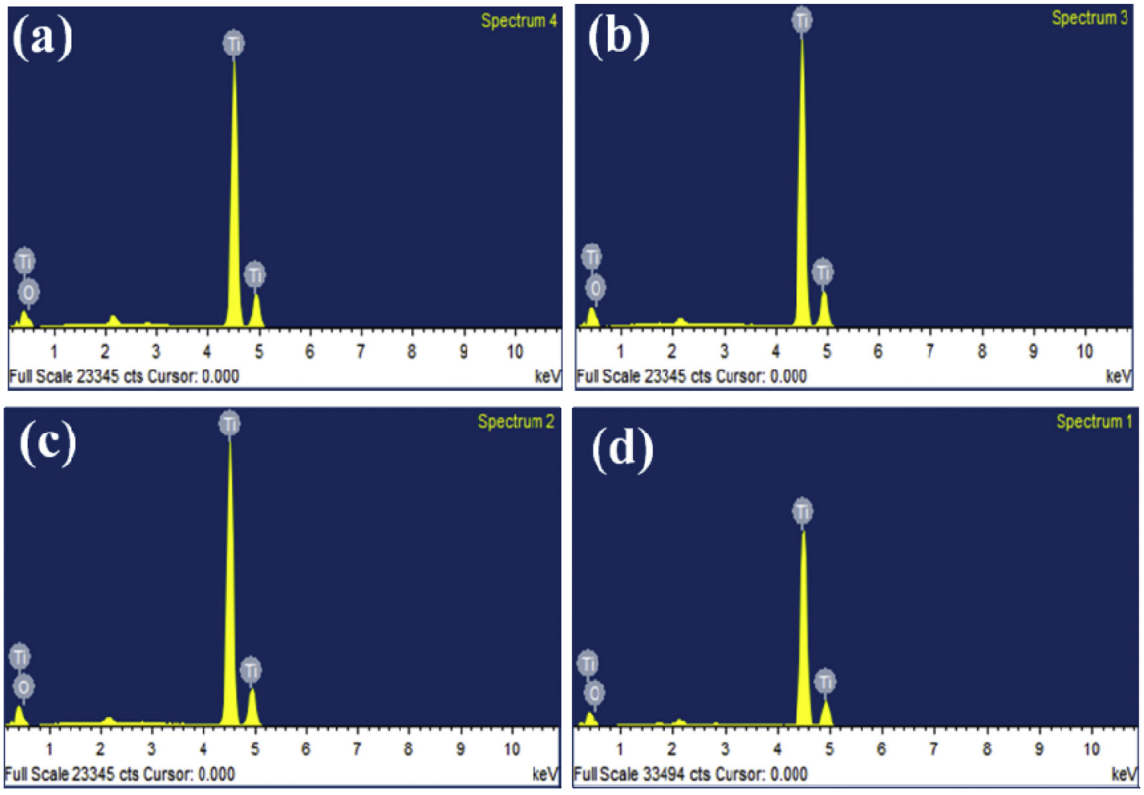

Fig. 3 – EDAX spectra of (a) 1, (b) 3, (c) 5 and (d) 7 min cathodized defect rich titania nanostructure samples.

appeared at 463.7 eV (Ti^{3+}) and 465.1 eV (Ti^{4+}). On the other hand, the high-resolution peaks of the 7 min cathodization sample obtained at 458.4 eV (Ti^{3+}) and 458.9 eV (Ti^{4+}) for $Ti2p_{3/2}$ level, as shown in Fig. 6c. The $Ti2p_{1/2}$ binding energy is presented at 463.4 eV (Ti^{3+}) and 464.7 (Ti^{4+}) (Fig. 6c). In the 7 min cathodization sample, the shift of binding energy of Ti^{3+} and (Ti^{4+}) state has confirmed the presence of oxygen vacancies in TiO_2 nanostructure. Furthermore, the XPS result of O1s in TiO_2 nanostructure (1 min) was obtained at 530.3, 530.8 and 531.9 eV for TiO_2 bonding structure, as shown in Fig. 6b. Fig. 6d shows that the high-resolution O1s peaks of TiO_2 nanostructure (7 min) are presented at 529.8, 530.6, 531.2 and 532 eV for Ti^{4+}, TiO_2, Ti_2O_3 and Ti–O–OH, respectively. The O1s XPS result is confirmed the oxygen vacancies in the 7 min catherization sample. In addition, oxygen vacancies are confirmed by EPR studies in Fig. S4.

3.6. *Electrochemical studies*

3.6.1. *Electrochemical impedance spectroscopy (EIS)*

Electrochemical impedance spectroscopy (EIS) is a powerful analysis technique to detect the changes in the interfacial properties of the electrode surface and electrolyte reaction. It can regulate both the resistive and capacitive (dielectric) features of the material. The impedance spectrum is acquired by varying the frequency over a wide range of alternating current (AC). The AC signal has amplitude of 10 mV in the frequency range from 0.1 to 105 Hz at zero DC bias in the dark. To further clarify charge transport features of the prepared defect rich titania nanostructure samples, the EIS is carried out by sweeping the frequency from 100 kHz to 1 mHz with a AC amplitude of 10 mV at an ambient temperature. The Nyquist plot (Fig. 7) is fitted using EC- lab software. On fitting, the 'Rct' response is partially lost and 'C' is enhanced as the Ti reduces to defect-rich titania nanostructure on cathodization. Moreover, the semicircle diameter of the 7 min cathodized sample is less than that of other cathodization samples, as shown in

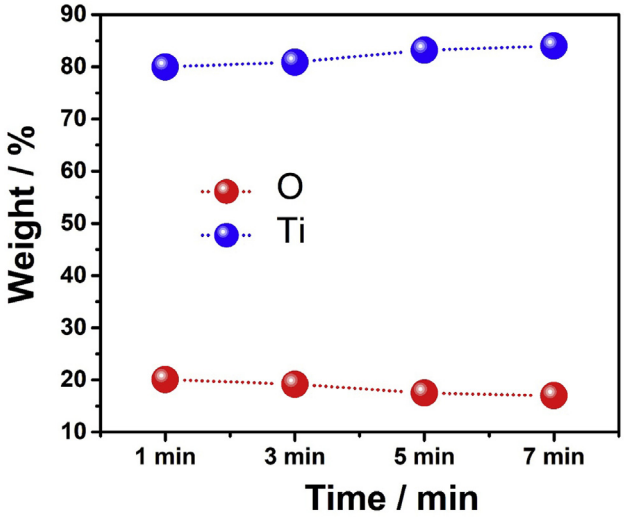

Fig. 4 – EDAX for weight % and atomic % of (a) 1, (b) 3, (c) 5 and (d) 7 min cathodized the defect rich titania nanostructure samples.

Fig. 7. In continuous, the resistance values are found out in Table 1. The resistances are 45093, 40174, 39708 and 11206 Ω for 1, 3, 5 and 7, respectively. From the Nyquist plot, the 7 min cathodization shows a high conductivity compared to other samples. Moreover, the decreased resistance in defect-rich titania nanostructure is explained by the crystalline growth, oxygen-deficient (reducing band-gap) [24], and electrically conducting oxide defect rich titania nanostructure. Because the quantity and mobility of charge carriers can be boosting the efficacy of interfacial reactions in HER reaction, these results confirmed the large charge carrier concentration with high electron mobility in defect-rich titania nanostructure (7 min) compared to other samples.

Table 1 – The resistance value of 1, 3, 5 and 7 min cathodization defect rich titania nanostructure samples.

Time of Cathodization (min)	Resistance Value (Ω)
1	39,708
3	40,174
5	45,093
7	**11,206**

3.6.2. *HER study*

Linear sweep voltammetry (LSV) is a voltammetry technique where the current at a working electrode is measured while the potential between the working electrode and a reference electrode is swept linearly in time. The electrochemical experiments were evaluated at room temperature employing an electrochemical system (SP-150, Biologic science instruments, France). A classical 3-electrodes setup with platinum as the counter electrode, a saturated calomel as the reference electrode and the cathodized defect-rich titania nanostructure as the working electrode was used.

A set of detailed essential electrochemical characterizations that include LSV, Tafel analysis, impedance spectroscopy and stability studies were carried out to elucidate the defect-rich titania nanostructure for HER in the solution of 1 M sulphuric acid. Fig. 8A shows the linear sweep voltammogram for the cathodized samples for the various time intervals (1, 3, 5 and 7 min). It is linearly swept across the potential range of −1.0 to 0.2 V vs. RHE (reversible hydrogen electrode) with a scan rate of 10 mV/s. From the studies, it can be confirmed that 7 min sample shows a good catalytic activity compared to other samples. Fig. 8A shows a current density of −68, −100, 135, and −150 mA/cm^2 at onset potential of −0.8, −0.39, −0.37 and −0.17 V in 1 M sulphuric acid for 7 min cathodized samples, respectively. Moreover, the value of obtained Turn Over Frequency (TOF) is 1.956*10^{-4} s^{-1} at −0.25 V *vs* RHE for 7 min sample. The result of defect rich titania nanostructure (7 min) showed that it is comparable to Pt. Fig. 8B shows the comparison of the prepared the defect-rich titania nanostructure with the noblest catalyst Pt and insert comparison of HER activity of 7 and 9 min, increasing onset potential for 9 min due to reducing oxygen-deficient higher cathodization time. Furthermore,

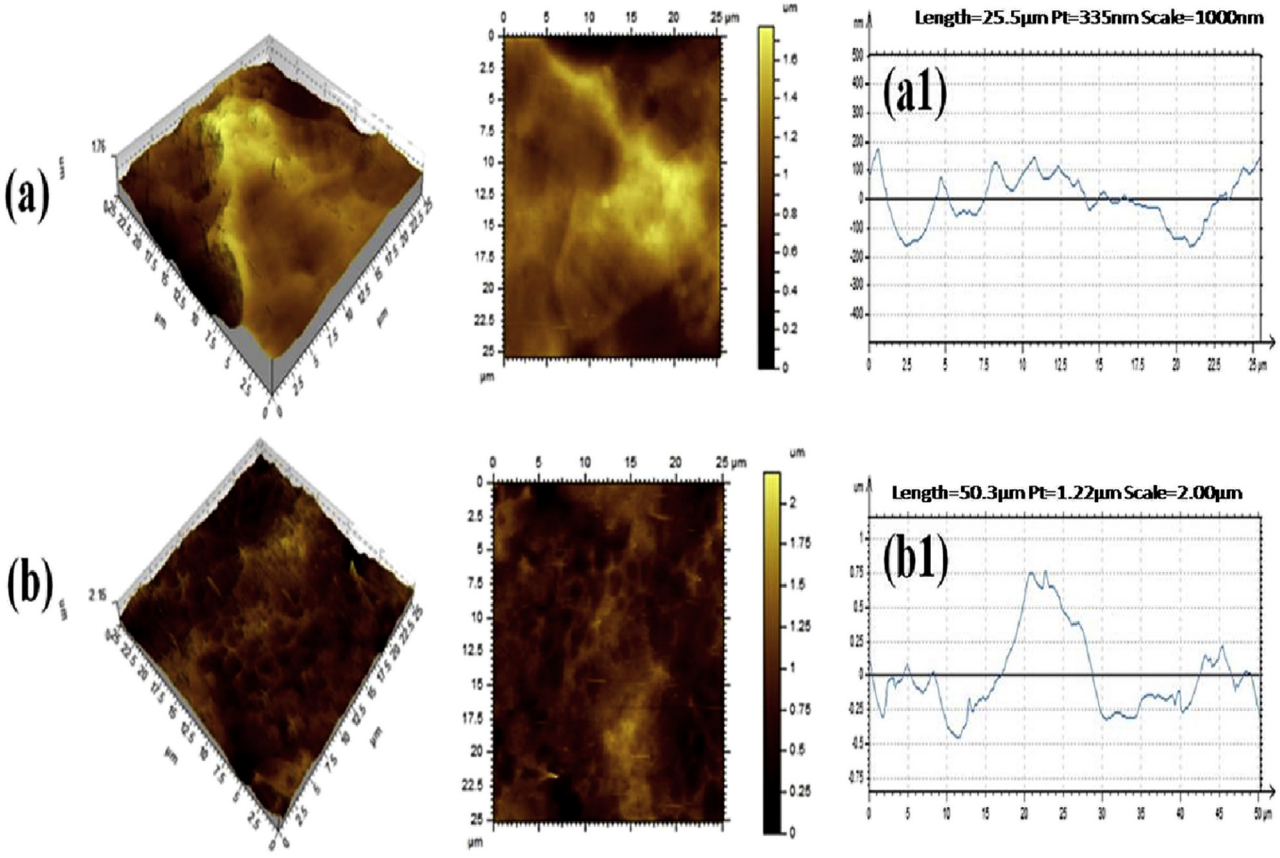

Fig. 5 – AFM topographical (a) 2D and (b) 3D images for cathodized1 and 7 min defect rich titania nanostructure sample, respectively. (a1) and (b1) show the roughness factor values of 1 and 7 min sample.

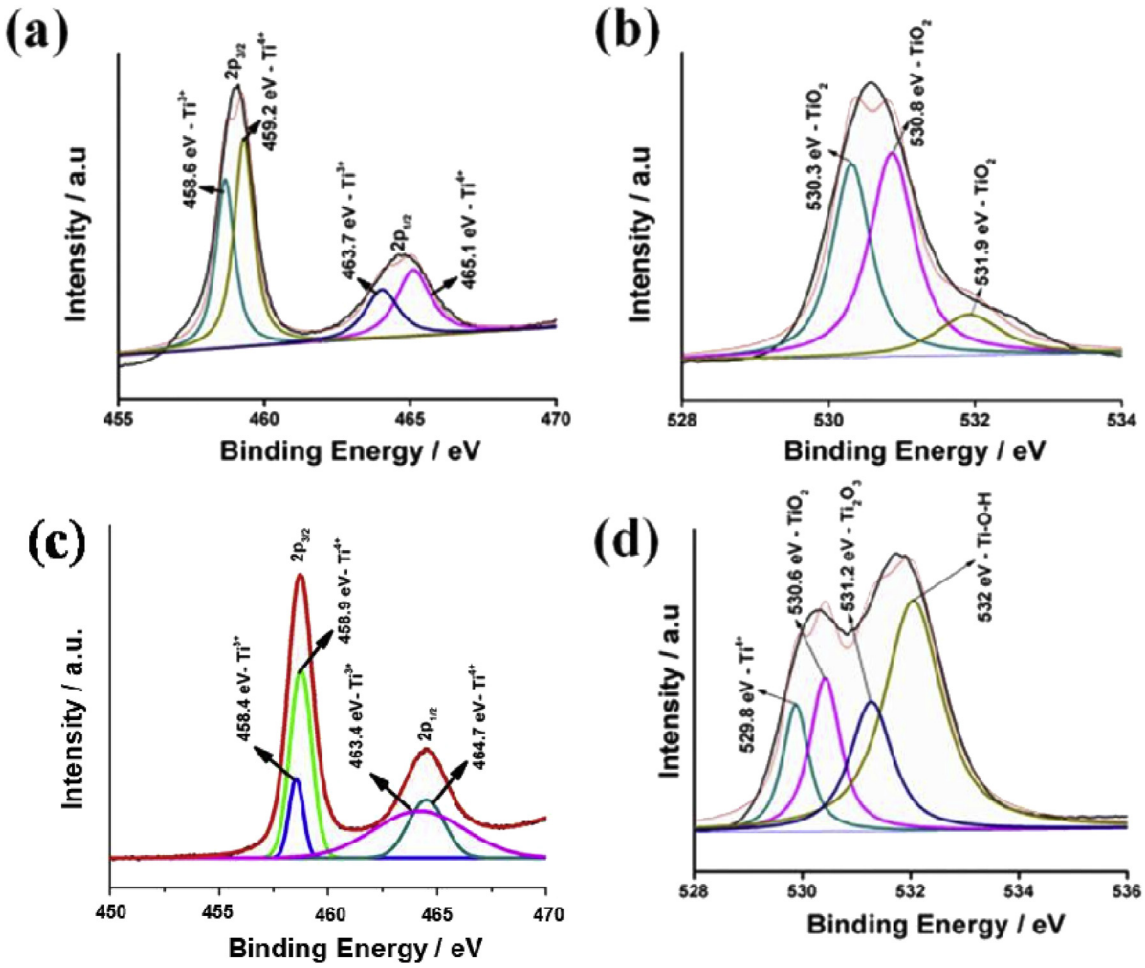

Fig. 6 – High resolution XPS spectra of (a) Ti2p & (b) O1s for 1 min and (c) Ti2p & (d) O1s 7 min cathodized defect rich titania nanostructure samples.

Table 2 shows the onset potential and current density of the corresponding samples. Further, the comparison of HER performance of various titania-based electrocatalysts shows in Table S1.

3.6.3. *Tafel slope determination*

Tafel curves were obtained for voltage (V) vs log j (mA/cm^2). Fig. 8C shows the Tafel curves of all cathodized samples with the Tafel slope of 0.1528, 0.2129, 0.1588 and 0.0938 V dec^{-1} for

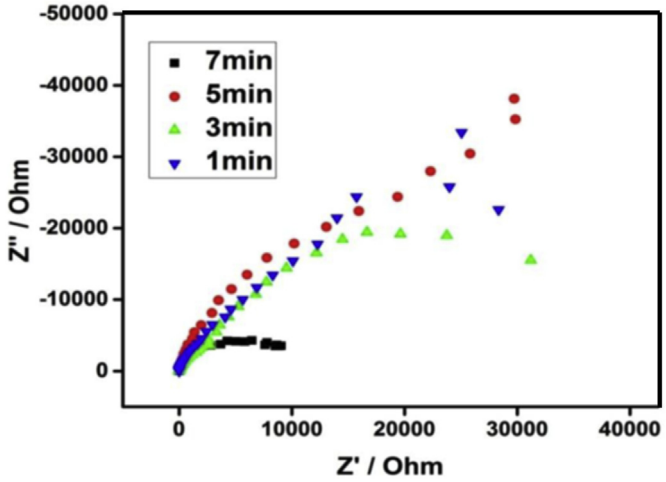

Fig. 7 – EIS for 1, 3, 5 and 7 min cathodized defect rich titania nanostructure samples.

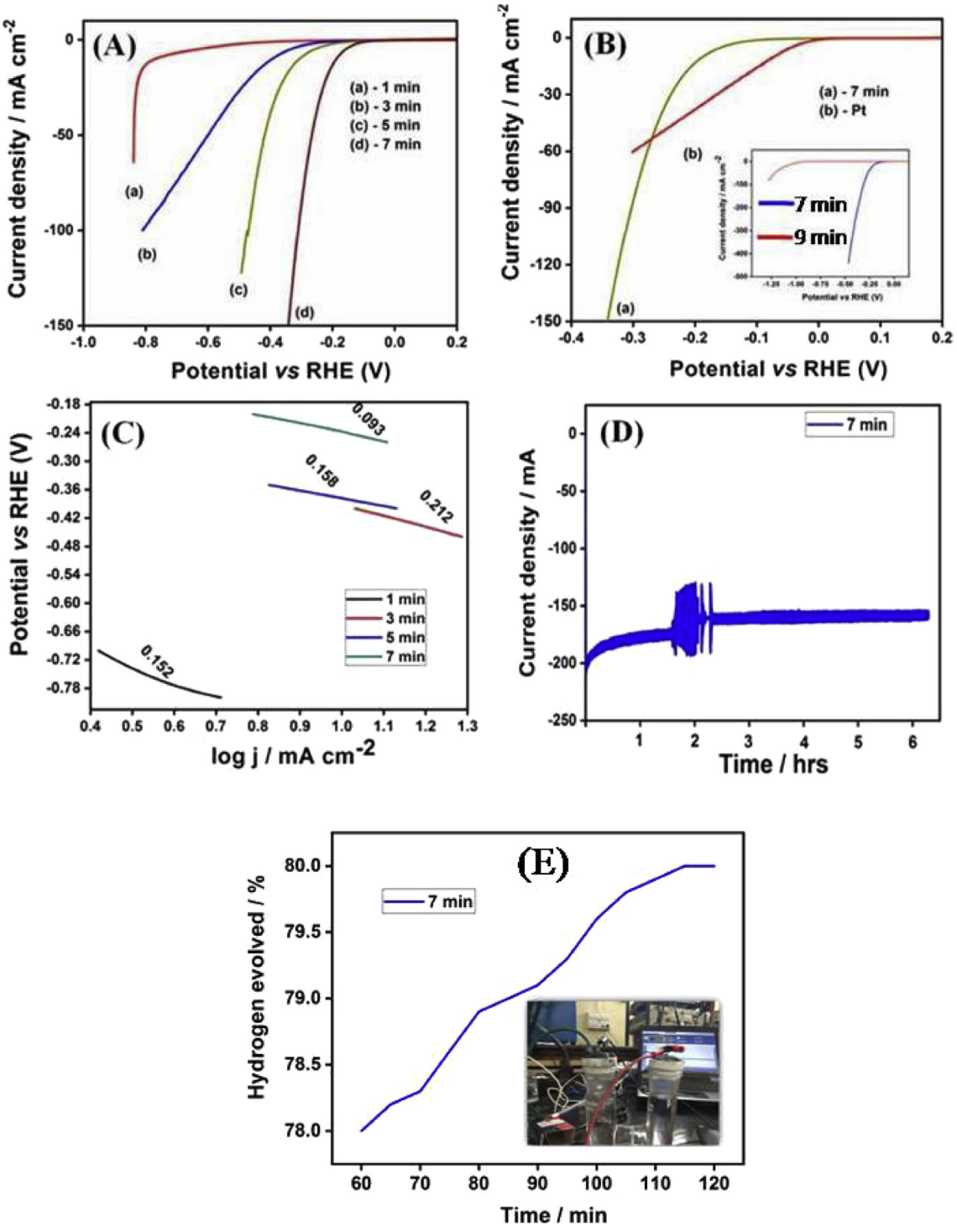

Fig. 8 – A. Polarization results for (a) 1, (b) 3, (c) 5 and (d) 7 min cathodized defect rich titania nanostructure samples in 1 M H_2SO_4 aqueous electrolyte with scan rate of 0.010 V s^{-1} for HER. B. HER activity studies for a) 7 min cathodized defect rich titania nanostructure sample and b) Pt, and insert image show the HER activity of 7 and 9 min sample. C. Tafel slope for 1, 3, 5 and 7 min cathodized defect rich titania nanostructure samples. D. Stability test for 7 min cathodized defect rich titania nanostructure sample. E. The collection of hydrogen gas (in percentage) was investigated using hydrogen sensor for 7 min defect rich titania nanostructure.

Table 2 – Onset potential and current density of cathodized samples for HER.

Cathodization time (minutes)	Onset potential (V)	Current density ($mA/cm^{2)}$
1	−0.8	−68
3	−0.39	−100
5	−0.37	−135
7	**−0.17**	**−150**

1, 3, 5 and 7 min, respectively. It is clear from the Tafel slope that 7 min sample outperforms all the other three samples by providing the slope value of 0.0938 V dec^{-1}, which is a very low value. The high exchange current density and low Tafel slope of the defect-rich titania nanostructure are rationalized by the presence of massive point defects and hence more active sites are created for improving HER performance.

3.6.4. *Chronoamperometry study*

Since a tremendous enhancement of activity was noticed during cathodization, the defect-rich titania nanostructure is demonstrated as significant HER in-activity in an acidic medium. As the catalyst activity is accelerated under the reaction conditions (acidic) of HER, it is beneficial to achieve a stable performance during electrolysis. To probe the extended electrochemical stability, the chronoamperometric electrolysis is

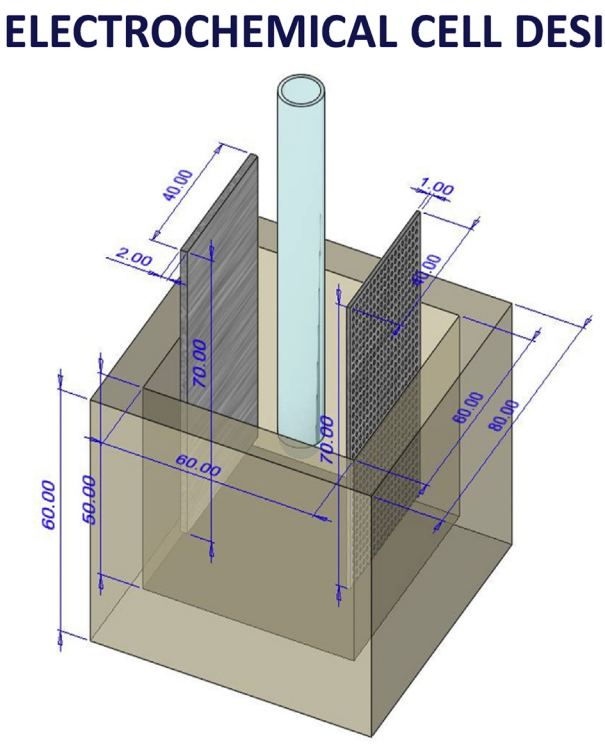

Fig. 9 – Electrochemical Cell Design for two-electrode water electrolyzer.

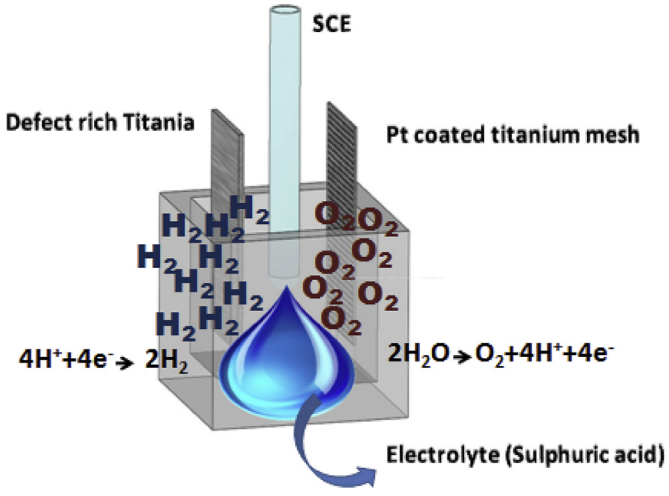

Fig. 10 – Mechanism of Water splitting.

Table 3 – Cost estimation of cell.

Materials	Amount	Cost INR
Ti plate	1 piece (5.5 × 1 sq.cm)	70
Nitric acid	25 ml	16.5
Hydrofluoric acid	5 ml	6
Sulphuric acid	10 ml	9
Cell container	100 ml	100
Pt coated Ti mesh	5.5 × 1 sq.cm	40
Total Cost:		**241.5 (approx)**

carried out for 7 min sample under a static potential of 1.2 V vs SCE, which shows a stable current density of 2.5 mA cm^{-2} for almost 6 h (Fig. 8D). After 6 h reason, the current density was reduced due to the deformation the morphology, shown in Fig. S1 (a & b). The hydrogen efficiency could be investigated using a hydrogen sensor with the water electrolyzer for 7 min defect-rich titania nanostructure electrocatalyst (Fig. 8F). The collection efficiency is 80% in 1 M sulphuric acid solution.

3.6.5. *Large scale study*

As we have carried out the experiments to the laboratory scale level, it is important to perform experiments on a large scale. We have exposed the 4 × 2.5 cm^2 area of prepared the defect rich titania plate and have studied LSV and its stability. The designing of an electrochemical cell plays a vital role. Figs. 9 and 10 show the electrochemical cell design, which is used for the water oxidation reaction. We have carried out linear sweep voltammetry where the conventional two-electrodes setup, with platinum as the counter electrode and the cathodized defect-rich titania nanostructure as the working electrode, was used. The cathodized 7 min sample has shown a good onset potential and current density. It can be concluded that cathodized defect-rich titania nanostructure can be well used for electrocatalytic hydrogen evolution reaction, which provides effective results in the acidic medium. The total cost estimation of the water electrolyzer cell has been presented in Table 3.

4. Conclusions

In summary, we have successfully demonstrated a feasible electrochemical cathodization method to prepare highly HER active electrocatalyst. The modified defect-rich titania nanostructure showed an excellent electrochemical performance which was demonstrated by the stability, Tafel slope, and onset potential. The prepared electrocatalyst exhibited a lower onset potential of −0.17 V V RHE and current density of −150 mA cm^{-2} to drive a HER performance. Moreover, the defect rich titania had shown a facile kinetics for HER in 1 M sulphuric acid by showing the Tafel slope of 0.0938 V dec^{-1}. The result of the complete cell characterization showed that the defect-rich titania was an extremely stable for HER activity in acidic conditions which was mainly attributed to the high corrosion resistance. The encouragement of the highly positive results of the overall study implied that the defect-rich TiO_2 could be chosen as the cost-effective and stable electrocatalytic electrode material for the large-scale water electrolysis in the future of hydrogen fuel production. The prepared defect-rich titania could be swapped the expensive materials like Pt, Ir and Ru to reduce the cost of hydrogen production.

Declaration of Competing Interest

The authors declare that they have no known competing financial interests or personal relationships that could have appeared to influence the work reported in this paper.

Acknowledgement

The authors extend their appreciation to the Deanship of Scientific Research, King Saud University for funding this work through Research Group no RG-1441-043 and funded by the Taif University Researchers Supporting Project number (TURSP-2020/04), Taif University, Taif, Saudi Arabia. One of the author Dr G. Murugadoss would like to thank Chancellor, President and Vice Chancellor, Sathyabama Institute of Science and Technology, Chennai for providing lab facilities and encouragement.

Appendix A. Supplementary data

Supplementary data to this article can be found online at https://doi.org/10.1016/j.jmrt.2021.07.119.

REFERENCES

[1] Kannan MW, Nocera DG. In situ formation of an oxygen-evolving catalyst in neutral water containing phosphate and Co^{2+}. Science 2008;321:1072.
[2] Liang Y, Li Y, Wang H, Zhou J, Wang J, Regier T, et al. Co_3O_4 nanocrystals on graphene as a synergistic catalyst for oxygen reduction reaction. Nat Mater 2011;10:780.
[3] McCrory CCL, Jung S, Peters JC, Jaramillo TF. Benchmarking heterogeneous electrocatalysts for the oxygen evolution reaction. J Am Chem Soc 2013;135:16977.
[4] Zhang L, Wen X, Kong T, Zhang L, Gao L, Miao L, et al. Preparation and mechanism research of Ni-Co supported catalyst on hydrogen production from coal pyrolysis. Sci Rep 2019;9:9818.
[5] Melis A, Happe T. Hydrogen production, green algae as a source of energy. Plant Physiol 2001;127:740.
[6] Vagia EC, Lemonidou AA. Hydrogen production via steam reforming of bio-oil components over calcium aluminate supported nickel and noble metal catalysts. Appl Catal A Gen 2008;351:111.
[7] Sun Y, Nakano J, Liu L, Wang X, Zhang Z. Achieving waste to energy through sewage sludge gasification using hot slags: syngas production. Sci Rep 2015;5:11436.
[8] Buscema M, Island JO, Groenendijk DJ, Blanter SI, Steele GA, van der Zant HSJ, et al. Photocurrent generation with two-dimensional van der Waals semiconductors. Chem Soc Rev 2015;44:3691.
[9] Anantharaj S, Karthick K, Venkatesh M, Simha TVSV, Salunke AS, Ma L, et al. Enhancing electrocatalytic total water splitting at few layer Pt-NiFe layered double hydroxide interfaces. Nanomater Energy 2017;39:30.

[10] Malik B, Anantharaj S, Karthick K, Pattanayak DK, Kundu S. Magnetic CoPt nanoparticle-decorated ultrathin $Co(OH)_2$ nanosheets: an efficient bi-functional water splitting catalyst. Catal Sci Technol 2017;19:16.
[11] Macak JM, Zlamal M, Krysa J, Schmuki P. Self-organized TiO_2 nanotube layers as highly efficient photocatalysts. Small 2007;3:300.
[12] Gratzel M. Photoelectrochemical cells. Nature 2001;414:338.
[13] Varghese OK, Gong D, Paulose M, Ong KG, Dickey EC, Grimes CA. Extreme changes in the electrical resistance of titania nanotubes with hydrogen exposure. Adv Mater 2003;15:624.
[14] Ahmad I, Shah SM, Zafar MN, Ashiq MN, Tang W, Jabeen U. Synthesis, characterization and charge transport properties of Pr–Ni Co-doped $SrFe_2O_4$ spinel for high frequency devices applications. Ceram Int 2021;47:3760.
[15] Ahmad I, Shah SM, Zafar MN, Ullah S, Ul-Hamid A, Ashiq MN, et al. Fabrication of highly resistive La-Zn co-substituted spinel strontium nanoferrites for high frequency devices applications. Mater Chem Phys 2021;259:124031.
[16] Xie J, Gao L, Jiang H, Zhang X, Lei F, Hao P, et al. Platinum nanocrystals decorated on defect-rich MoS_2 nanosheets for pH-universal hydrogen evolution reaction. Cryst Growth Des 2019;19:60.
[17] Xie J, Qi J, Lei F, Xie Y. Modulation of electronic structures in two-dimensional electrocatalysts for hydrogen evolution reaction. Chem Commun 2020;56:11910.
[18] Xie J, Yang X, Xie Y. Defect engineering in two-dimensional electrocatalysts for hydrogen evolution. Nanoscale 2020;12:4283.
[19] Xie J, Qu H, Xin J, Zhang X, Cui G, Zhang X, et al. Defect-rich MoS_2 nanowall catalyst for efficient hydrogen evolution reaction. Nano Res 2017;10:1178.
[20] Xie J, Zhang H, Li S, Wang R, Sun X, Zhou M, et al. Defect-rich MoS_2 ultrathin nanosheets with additional active edge sites for enhanced electrocatalytic hydrogen evolution. Adv Mater 2013;25:5807.
[21] Xie J, Zhang J, Li S, Grote F, Zhang X, Zhang H, et al. Controllable disorder engineering in oxygen-incorporated MoS_2 ultrathin nanosheets for efficient hydrogen evolution. J Am Chem Soc 2013;135:17881.
[22] Xie J, Xie Y. Structural engineering of electrocatalysts for the hydrogen evolution reaction: order or disorder? ChemCatChem 2015;7:2568.
[23] Okamoto H. O-Ti (Oxygen-Titanium). J Phase Equilib Diffus 2011;32:473.
[24] Bartholomew RF, Frankl DR. Electrical properties of some titanium oxides. Phys Rev 1969;187:828.
[25] Bartkowski S, Neumann M, Kurmaev E, Fedorenko V, Shamin S, Cherkashenko V, et al. Electronic structure of titanium monoxide. Phys Rev B 1997;56:10656.
[26] Su Z, Zhou W. Formation, morphology control and applications of anodic TiO_2 nanotube arrays. J Mater Chem 2011;21:8955.
[27] Zhu K, Neale NR, Miedaner A, Frank AJ. Enhanced charge-collection efficiencies and light scattering in dye-sensitized solar cells using oriented TiO_2 nanotubes arrays. Nano Lett 2007;7:69.
[28] Fujishima A, Honda K. Electrochemical photolysis of water at a semiconductor electrode. Nature 1972;238:37.
[29] Wang R, Hashimoto K, Fujishima A, Chikuni M, Kojima E, Kitamura A. Light-induced amphiphilic surfaces. Nature 1997;388:431.
[30] Su Z, Zhou W. Formation, microstructures and crystallization of anodic titanium oxide tubular arrays. J Mater Chem 2009;19:2301.
[31] Allam NK, Shankar K, Grimes CA. A general method for the anodic formation of crystalline metal oxide nanotube arrays without the use of thermal annealing. Adv Mater 2008;20:3942.
[32] Feng H, Xu Z, Ren L, Liu C, Zhuang J, Hu Z, et al. Activating titania for efficient electrocatalysis by vacancy engineering. ACS Catal 2018;8:4288.
[33] Robin A, de Almeida Ribeiro MB, Rosa JL, Nakazato RZ, Silva MB. formation of TiO_2 nanotube layer by anodization of titanium in ethylene glycol-H_2O electrolyte. J Surf Eng Mater Adv Technol 2014;4:123.
[34] Kavan L, Stoto T, Graetzel M, Fitzmaurice D, Shklover V. Quantum size effects in nanocrystalline semiconducting titania layers prepared by anodic oxidative hydrolysis of titanium trichloride. J Phys Chem 1993;97:9493.
[35] Jayashree S, Ravichandran S, Vengatesan S. Defect-rich metallic titania ($TiO_{1.23}$) - an efficient hydrogen evolution catalyst for electrochemical water splitting. ACS Catal 2016;6:2222.
[36] Jayashree S, Ravichandran S. Insights into the electrocatalytic behavior of defect-centered reduced titania ($TiO_{1.23}$). J Phys Chem C 2018;122:1670.